

PASSIVE SCALAR AND SCALAR GRADIENT STATISTICS NEAR THE TURBULENT/NON-TURBULENT INTERFACE IN A SPATIALLY EVOLVING MIXING LAYER

Antonio Attili, Juan C. Cristancho & Fabrizio Bisetti

Clean Combustion Research Center,

King Abdullah University of Science and Technology, Kingdom of Saudi Arabia

Abstract An analysis of a passive scalar field in the vicinity of the turbulent/non-turbulent interface in a spatially evolving mixing layer is presented. A vorticity threshold is defined to detect the interface separating the turbulent from the non-turbulent regions of the flow. The passive scalar conditional mean is characterized by a strong jump near the interface. The strong jump for the scalar has been observed before in the case of high Schmidt number, but it is a new result for Schmidt number of order one. Finally, the scalar dissipation is characterized by a strong and narrow peak near the interface.

INTRODUCTION

In shear flows, such as jets, wakes, and mixing layers, the turbulent and irrotational regions are separated by a sharp interface [2]. The study of this interface has recently gained new attention [6]. This layer plays a crucial role in the development of the turbulent field and is important in turbulent combustion and cloud physics as it affects entrainment and mixing. Recent important results include new insight on the entrainment process, which is dominated by the spreading of small scale vortices [7, 8, 5] and on the characteristic thickness of the interface. The thickness is of the order of the Kolmogorov's scale in shear-free turbulence [5] and Taylor's microscale in flows with mean shear [3, 4]. In addition, a strong vorticity jump has been observed close to the interface for a number of free shear flows [3, 4, 8, 6].

In the present work, the turbulent/non-turbulent interface in a spatially evolving mixing layer is analyzed. The study is based on a recent Direct Numerical Simulation performed by the authors [1]. A Kelvin-Helmholtz instability develops starting from a laminar hyperbolic tangent profile having vorticity thickness $\delta_{\omega,0}$ at the inlet and perturbed with low amplitude white noise. The computational domain, spanning the region $473\delta_{\omega,0} \times 290\delta_{\omega,0} \times 157.5\delta_{\omega,0}$ ($L_x \times L_y \times L_z$), is discretized with $3072 \times 940 \times 1024 \sim 3$ billion ($n_x \times n_y \times n_z$) grid points. The Reynolds number based on the vorticity (momentum) thickness at the inlet is $Re_\omega = 600$ (resp. $Re_\theta = 150$), increasing up to $Re_\omega = 25,000$ (resp. $Re_\theta = 4250$) as the mixing layer develops. In the fully developed region the Reynolds number based on the Taylor's microscale is around $Re_\lambda \approx 250$. A complete description of the flow parameters and methods used for the computation is given in [1], together with an analysis of the spatial evolution of the flow and velocity statistics in the transitional and fully developed turbulent regions.

DEFINITION OF THE TURBULENT/NON-TURBULENT INTERFACE

The interface between the turbulent and non-turbulent region has been defined using a threshold value for the vorticity magnitude. The threshold selected is around 30% of the mean vorticity in the core of the layer. Figure 1 shows the vorticity magnitude field in the streamwise/crosswise plane and the two interfaces between the core of the layer and the low- and high-speed irrotational regions (bottom and top, respectively). Both interfaces are highly convoluted and characterized by a wide range of length scales. It is worth noting that the two interface appear qualitatively different.

Following [7], [3], and [8], the interface *envelope* is defined using the outermost points of the interface along lines at a given streamwise location. Turbulence statistics are computed conditioned on the distance from the envelope. As suggested by [3], patches of engulfed irrotational fluid are removed from the statistics.

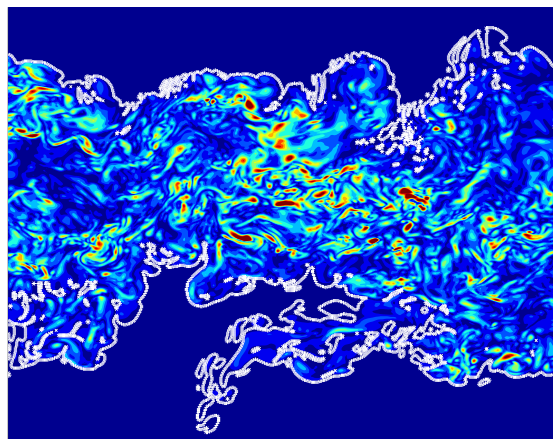


Figure 1. Vorticity magnitude in the self similar region. The threshold used to define the interface is also shown (white lines).

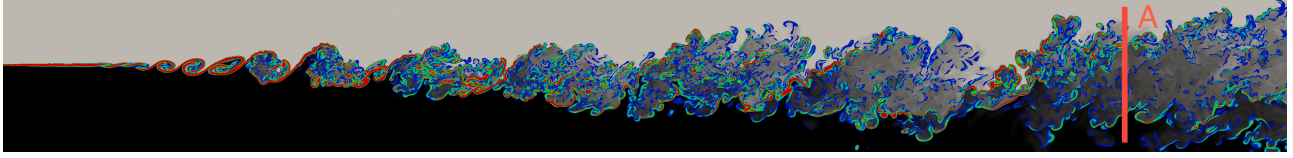


Figure 2. Passive scalar field (black and white) and passive scalar dissipation field (color). The scalar dissipation is shown only in regions where the value is larger than 0.015. The vertical red line indicates the streamwise position where the conditional statistics are computed.

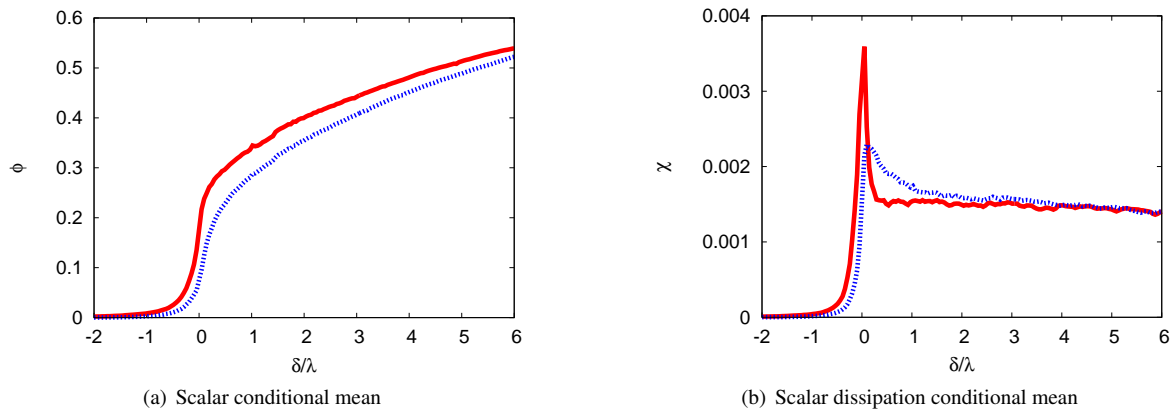


Figure 3. Passive scalar statistics conditioned on the distance from the interface in the streamwise position indicated by the letter A in figure 2. Red solid line: low-speed interface; blue dashed line: high-speed interface.

PASSIVE SCALAR CONDITIONAL STATISTICS

An overview of the scalar field is shown in figure 2. Figure 3(a) displays the average scalar conditioned on the distance from the interface. Results for the two interfaces, separating the core of the layer from the low- and high-speed irrotational sides, are shown. The distance is normalized by the Taylor’s microscale. The presence of a strong jump in the mean scalar is apparent, especially for the low-speed interface. The jump has been observed before by [8] in an experiment of a turbulent jet. The appearance of the jump was ascribed to the high Schmidt number (≈ 2000) characterizing the dye used as passive scalar in the jet experiment. For the first time, such a strong jump is observed for a scalar with $Sc \approx 1$. Figure 3(b) shows the conditional mean of the passive scalar dissipation. It is evident that the structures characterized by high scalar dissipation are concentrated in the external part of the layer, close to the turbulent/non-turbulent interface. The two interfaces display a remarkably different behavior. While on the low-speed side the dissipation has a large overshoot concentrated in a layer characterized by a thickness of few Kolmogorov’s lengths, the overshoot for the high-speed side is smaller and characterized by a larger thickness.

References

- [1] A. Attili and F. Bisetti. Statistics and scaling of turbulence in a spatially developing mixing layer at $Re_\lambda = 250$. *Phys. Fluids*, **24**(3):035109, 2012.
- [2] S. Corrsin and A.L. Kistler. Free-stream boundaries of turbulent flows. Technical Report TN-1244, NACA, Washington, DC, 1955.
- [3] C.B. da Silva and J.C.F. Pereira. Invariants of the velocity-gradient, rate-of-strain, and rate-of-rotation tensors across the turbulent/nonturbulent interface in jets. *Phys. Fluids*, **20**:055101, 2008.
- [4] C.B. da Silva and R.R. Taveira. The thickness of the turbulent/nonturbulent interface is equal to the radius of the large vorticity structures near the edge of the shear layer. *Phys. Fluids*, **22**:121702, 2010.
- [5] M. Holzner and B. Lüthi. Laminar superlayer at the turbulence boundary. *Phys. Rev. Lett.*, **106**(13):134503, 2011.
- [6] J.C.R. Hunt, I. Eames, C.B. da Silva, and J. Westerweel. Interfaces and inhomogeneous turbulence. *Philos. Trans. R. Soc. London, Ser. A*, **369**(1937):811–832, 2011.
- [7] J. Mathew and A.J. Basu. Some characteristics of entrainment at a cylindrical turbulence boundary. *Phys. Fluids*, **14**:2065, 2002.
- [8] J. Westerweel, C. Fukushima, J.M. Pedersen, and J.C.R. Hunt. Mechanics of the turbulent-nonturbulent interface of a jet. *Phys. Rev. Lett.*, **95**(17):174501, 2005.